Online ISSN: 2981-0396 Print ISSN: 2981-0388

International Journal of Iron & Steel Society of Iran

Journal Homepage: https://journal.issiran.com/

Research Article

CFD Analysis of Thermal Stress and Shear Stress in the First-Stage Feed-Gas Tube Bundle of a Midrex Recuperator: Critical Zone Identification

M. Salehi *[1], H. Soltani [2], M. Ehsani [3], H. farhadi [4]

Mechanical Engineering Group, Department of Engineering, South Kaveh Steel Co, Bandar Abbas, Iran

ARTICLE INFO

Keywords:

Direct Reduction of Iron, Recuperator, Reformer, Tube Bundle, Feed Gas.

Article history:

Received 04 September 2025
Received in revised form 03 February 2026
Accepted 11 May 2026

ABSTRACT

In the Midrex direct reduction process, the process gas is preheated by a recuperator made of a group of steel tubes, known as tube bundles, which work as a shell-and-tube heat exchanger. One of the key parts of this system is the first-stage feed-gas tube bundle, which is the main focus of this study. In this study, the thermal behavior and shear stresses in the feed-gas tube bundle were investigated to identify critical zones and inform design optimization. To this end, numerical simulations were conducted using Computational Fluid Dynamics (CFD), and the distributions of temperature, pressure, and local gradients along the flow path were analyzed. The results revealed that significant variations in temperature and pressure gradients cause a sharp increase in both shear and thermal stresses at the tube inlet region. These conditions are accompanied by intensified convective heat flux, and repeated thermal cycles lead to thermal and thermo-mechanical fatigue at high tube-bundle operating temperatures. Over the long term, this fatigue mechanism promotes crack initiation in the inlet region, followed by local wall thinning, leakage, and progressive structural degradation. Validation of the numerical results through field inspection of damaged samples confirmed the existence of these critical regions. Based on these findings, the appropriate selection of geometry and structural materials is crucial to enhancing the reliability, efficiency, and safety of heat exchangers in direct reduction processes.

1. Introduction

The heat recovery section (Recuperator) is a key component for optimizing energy consumption and improving overall plant efficiency in the direct reduction of iron using the Midrex process. This unit consists of two parallel, similar flow paths, each comprising a bundle of steel tubes, referred to as a tube bundle. The recuperators operate as gas-to-gas heat exchangers, using the thermal energy of the hot flue gases from the reformer burners to preheat the process gas stream entering the reduction furnace to the desired temperature. In this system, the heated air produced by the combustion of the reformer burners enters the recuperator at approximately 1100°C and exchanges heat with the feed gases preheating within the tube bundles. This preheating process reduces fossil fuel consumption and improves the thermodynamic conditions of the reduction reactions, thereby enhancing overall system efficiency. The arrangement of the tube bundles in the recuperator includes the hot-air section, the second-stage feed gas, the first-stage feed gas, natural gas, and finally the cold-air section. Refractory linings

* *Corresponding Author*
Email: m.salehi@sksco.ir
Address: Mechanical Engineering Group, Department of Engineering, South Kaveh Steel Co, Bandar Abbas, Iran
1. M.S.c, 2. M.S.c, 3. M.S.c , 4. M.S.c

DOI: http://10.22034/IJISSI.2026.2070833.1329
Published by ISSI (Iron & Steel Society of Iran)

protect the recuperator shell against high heat flux. At the same time, the tube bundles are designed and positioned at different locations to regulate and control the temperature profile and flow rate of the incoming streams. Among these, the first-stage feed-gas tube bundle serves as the entry section for the process feed gas, providing initial preheating. This section is subjected to high operating temperatures and considerable thermal gradients. The tubes in this zone are made of stainless steel grade 1.4541 (AISI 321), which provides adequate resistance against oxidation and creep at elevated temperatures. Nevertheless, under long-term operating conditions, the tubes are subjected to severe thermal stresses and steep temperature gradients, which may lead to wall thinning, perforation, or leakage.

Failure or shutdown of the tube bundles not only entails significant replacement costs but also disrupts reformer operation and halts the reduction process, potentially causing severe damage to expensive equipment, such as reformer tubes. Therefore, extending the service life of tube bundles and preventing premature failures is of critical importance. In this context, the present study focuses on the design and performance analysis of the first-stage feed-gas tube bundle. The main objective is to identify critical thermal and mechanical zones and propose optimization strategies to enhance the equipment's service life. To achieve this, numerical simulations were performed using Computational Fluid Dynamics (CFD) with ANSYS Fluent 2022 R2, and the distributions of temperature, flow, and heat transfer along the flow path were investigated. These analyses provide a basis for design improvements and help enhance the reliability and efficiency of the system.

Extensive research has been conducted on the design, simulation, and optimization of recuperator-type heat exchangers. In 1987, Boone et al. [1] investigated the effects of fouling in gas turbine recuperators and demonstrated that deposit accumulation reduces thermal efficiency and increases pressure drop. In 1997, Medjukritskii et al. [2] employed computational models to simulate the influence of tube geometry and boundary conditions on heat transfer in recuperators, confirming the significance of these factors for the temperature distribution.

With advances in simulation techniques, CFD has become the primary tool for studying flow behavior and heat transfer in heat exchangers. In 2017, Wojciech Ludwig and Daniel Zajac [3] investigated geometric modifications to recuperators using CFD. They demonstrated that changes in tube arrangement can improve the uniformity of the temperature distribution and thermal efficiency. In the same year, Gupa [4] analyzed the effect of varying operating conditions, including inlet temperature and flow rate, on the performance of a gas turbine recuperator and identified their direct influence on thermal efficiency.

In addition, numerous studies have examined the design and analysis of ceramic heat exchangers and finned surfaces. For instance, in 2008, Chun Heesang simulated the thermal performance and thermal stresses of ceramic recuperators made of silicon carbide (SiC) and refractory alumina–mullite–spinel composites, demonstrating that material selection and wall thickness directly affect the temperature distribution and structural stability [5]. In 2018, Yang et al. confirmed through experimental investigations on ceramic recuperators that heat transfer is significantly enhanced at elevated temperatures [6]. Furthermore, in 2016, Krzysztof simulated the growth of deposits on recuperator tubes in industrial furnaces and showed that fouling can reduce thermal efficiency and induce pressure drop [7]. Collectively, these studies have provided a solid foundation for the thermal and mechanical analysis of tube bundles and highlight the importance of optimal design and material selection in improving the performance and durability of recuperators.

Recent research has primarily focused on advanced numerical analysis, geometric optimization, and operational conditions of recuperators. For example, in 2019, Marchionni et al. [8] modeled the transient behavior of printed recuperators and demonstrated that transient thermal variations significantly affect the exchanger's temperature response. In 2016, Patankar et al. [9] evaluated the design and performance of a compact recuperator for micro gas turbines and found that optimizing the tube geometry improves thermal efficiency. In 2019, Jimin et al. [10] employed a porous-medium model to simulate flow and heat transfer in U-tube heat exchangers, providing more accurate predictions of temperature distribution and pressure drop. In industrial applications, Shi (2018) [11] modeled transient recuperators for waste-heat recovery in steel production and highlighted the critical importance of transient temperature response in process control. Likewise, Ghanbarpour and Toghraee (2021) [12] simulated CHP systems equipped with recuperators, reporting performance optimization and energy efficiency estimation. Furthermore, Hussein et al. (2020) [13] applied artificial neural networks to predict the performance of gas turbine recuperators, showing that intelligent models can deliver accurate and rapid results. Despite these advancements, in industrial practice, the lack of a clear, quantitative identification of critical regions within tube bundles often leads to generalized design assumptions and non-targeted material or geometric modifications, which may fail to address the root causes of localized damage. The novelty of the present study lies in providing a focused and validated numerical framework for systematically identifying thermo-mechanically sensitive zones in the first-stage feed-gas tube bundle of a Midrex recuperator. By correlating local flow characteristics, thermal gradients, and stress indicators, this work enables the precise localization of damage-prone regions, particularly at the header-to-tube inlet transition. Such targeted identification of critical zones offers a more reliable

basis for design optimization, material selection, and service-life extension, thereby bridging the gap between numerical analysis and practical failure prevention in industrial tube-bundle systems.

2. Research Methodology

2.1. Problem Definition

In this study, the geometric modeling of the tube bundle for the first-stage feed-gas section of the recuperator system was performed in Autodesk Inventor 2022, based on actual operational data from the Kaveh South Kish Steel Plant.

Boundary conditions, including mass flow rate, inlet and outlet temperatures, absolute pressure, and other operational parameters, were determined from field measurements and the system's design specifications. Numerical analysis of flow and heat transfer within the tube bundle was conducted using ANSYS Fluent 2022 R2. The simulation was based on the numerical solution of the Navier–Stokes equations for compressible, viscous, and steady flow, coupled with the energy equation.

Validation was carried out using a damaged sample of the first-stage feed-gas tube bundle from the Kaveh South Kish Steel Plant.

2.2. Geometry of the Feed-Gas Tube Bundle

The three-dimensional geometry of the first-stage feed-gas tube bundle of the recuperator was redesigned and modeled in Autodesk Inventor 2022 based on actual operational data and available engineering drawings. In this modeling, key dimensions, including tube length, outer diameter, longitudinal and transverse spacing between tubes, and the total number of tubes in the array, were taken into account to replicate conditions as close as possible to the real process. The resulting 3D design and the main dimensions of the tube bundle are illustrated in Fig. 1.

2.3. Operating Parameters

The operating parameters used in this simulation were determined from the recuperator design data listed in Table 1. and applied as shown in Fig. 2.

2.4. Meshing

The mesh was generated for both the solid metallic structure and the fluid domain within the tubes, with a characteristic element size of 0.03m. This meshing strategy resulted in 1,089,522 nodes and 3,372,021 elements in the solid domain, and 1,848,170 nodes and 7,613,605 elements in the fluid domain. The numerical results for the outlet fluid temperature were subsequently validated against the actual operating conditions of the tube bundle, showing good agreement and were therefore considered acceptable.

2.5. Governing Equations

The governing equations used in the simulation include:

Continuity Equation (Mass Conservation):

$$\nabla \cdot V = 0 \qquad \text{Eq.(1)}$$

where ρ denotes the fluid density and ν represents the velocity vector. This equation enforces mass conservation throughout the computational domain.

Momentum Equation:

Eq.(2)

$$\frac{\partial(\rho\vec{v})}{\partial t} + \vec{\nabla}\cdot\left(\rho\vec{V}\vec{V}\right) = -\vec{\nabla}p + \vec{\nabla}\left(\mu\vec{\nabla}\vec{V}\right) - \vec{g}.\vec{x}\nabla\rho + \vec{S}_V$$

In this equation, ρ presents the static pressure, $=\mu_{eff}+\mu_t\mu$ indicates the effective viscosity accounting for both molecular and turbulent contributions, g shows the gravitational acceleration vector, and F represents additional body forces. The momentum equation describes the balance between inertial, pressure, viscous, and body forces acting on the fluid.

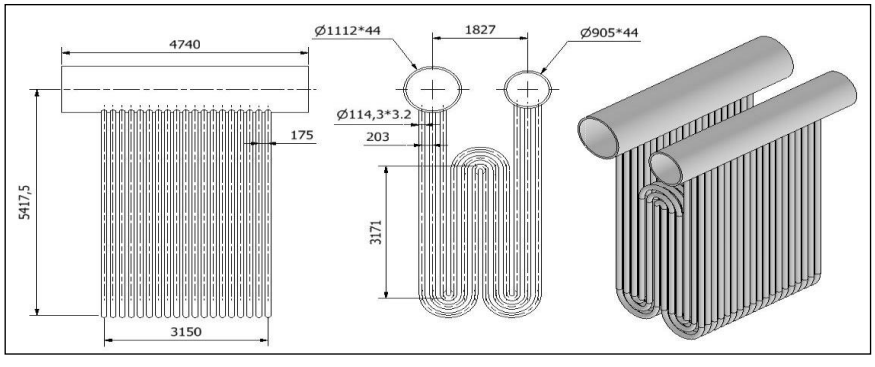

Fig. 1. Geometric dimensions of the first-stage feed-gas tube bundle.

Table 1. Operating parameters of the first-stage feed-gas tube bundle.

Gas Stream	Pressure	Temperature	Flow rate
Inlet gas to the first-stage feed-gas tube bundle	170000 Pa	141°C	139000 Nm^3/h
Outlet gas from the first-stage feed-gas tube bundle	164000 Pa	422°C	139000 Nm^3/h
Recuperator inlet gas from the first-stage feed-gas tube bundle region	-200 Pa	741°C	203000 Nm^3/h
Recuperator outlet gas from the first-stage feed-gas tube bundle region	-200 Pa	517°C	203000 Nm^3/h

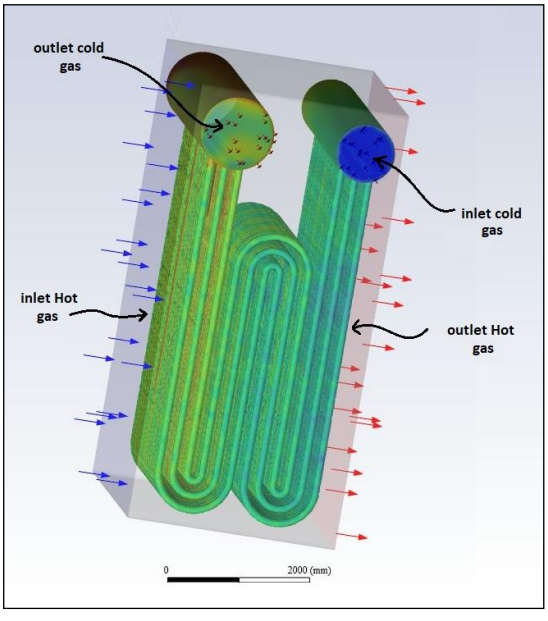

Fig. 2. Operating conditions of the first-stage feed-gas tube bundle.

The energy conservation equation is expressed as follows:

$$\nabla \cdot (\vec{v}\rho h) = \nabla . (k\, \nabla T) \qquad \text{Eq.(3)}$$

Here, h denotes the specific enthalpy, T is the temperature, and k_{eff} represents the effective thermal conductivity of the fluid. This equation governs the transport of thermal energy within the flow field.

The turbulent kinetic energy (k) represents the amount of energy contained in the flow fluctuations or turbulence and is expressed by the following equation:

Eq.(4)

$$\frac{\partial(\rho k)}{\partial t} + \frac{\partial(\rho v_i k)}{\partial x_i} = \frac{\partial}{\partial x_j}\left|(\mu + \frac{\mu_t}{\sigma_k})\frac{\partial k}{\partial x_j}\right| + G_k + \rho\varepsilon$$

$$\mu_t = \rho C_\mu \cdot \left(\frac{k^2}{\varepsilon}\right) \qquad \text{Eq.(5)}$$

In this formulation, k indicates the turbulent kinetic energy, μ_t presents the turbulent viscosity, σ_k is the turbulent Prandtl number for k, G_k represents the production of turbulent kinetic energy due to mean velocity gradients, and ε is the turbulent dissipation rate.

The above governing equations were solved using the finite volume method implemented in ANSYS Fluent.

2.6. Boundary Conditions

Air flow on both sides of the tube bundle (inside the tubes and on the shell side) was considered single-phase, compressible, and turbulent.

The Realizable k–ε turbulence model was employed due to its widespread application and proven accuracy in validated heat exchanger studies, with Standard Wall Functions used for near-wall treatment.

The outlet boundary for both sides of the flow was defined as Outflow.

Inlet boundaries were specified as Mass-Flow Inlet, with prescribed mass flow rates and temperatures.

Tube walls were modeled as Coupled Walls to enable conjugate heat transfer between the tube interior and exterior. Tube thickness and thermal properties were assigned in accordance with the design specifications.

The external shell and other model walls were treated as adiabatic surfaces with zero heat flux (Heat Flux = 0) to prevent heat exchange with the surrounding environment.

A no-slip boundary condition was applied to all walls.

Gravitational acceleration was set to 9.81 m/s^2.

A Pressure-Based solver with the Coupled algorithm was selected to discretize the momentum and pressure equations to solve the equations.

Temporal convergence was achieved when the residuals fell below 10^{-4}.

Thermodynamic properties of the fluid (air) were calculated using the Ideal Gas model with temperature-dependent properties.

The thermo-mechanical analysis has been performed

using a coupled FSI approach. The transfer of wall temperature fields from CFD to the structural model, along with the structural analysis setup and von Mises stress evaluation, has been incorporated into the Methodology section.

3. Results and Discussion

3.1. Analysis of Surface Shear Stresses in the Feed-Gas Tube Bundle

As shown in Fig. 3. the fluid undergoes abrupt changes in flow direction and cross-sectional area in the vicinity of the air inlet header and the flow transition from the header into the tubes. These geometric discontinuities promote flow separation, local turbulence, and jet impingement on the tube walls, resulting in steep velocity gradients and consequently elevated wall shear stress (WSS) on the inner surfaces of the tubes. Simultaneously, the outer surfaces of the tubes are exposed to high-temperature gas, while the incoming feed gas cools the inner surfaces. As a result, the temperature gradient across the tube wall reaches its maximum in this region. This pronounced thermal gradient leads to significant spatial variations in fluid properties and imposes severe thermal loading on the tube material. Although wall shear stress is a fluid-dynamic quantity, the combined action of high WSS (fluid-induced surface loading) and strong thermal gradients (thermally induced expansion mismatch) generates intensified mechanical loading within the tube material. These coupled thermal and fluid-induced loads were transferred to the structural domain and subsequently resulted in elevated equivalent von Mises stresses in the solid tubes, as illustrated in Fig. 4. The maximum WSS in this region is approximately 45 Pa, and its spatial coincidence with the maximum temperature gradient leads to the most severe thermo-mechanical loading, consistent with the structural stress distribution in Fig. 4. Therefore, the inlet header–to–tube transition region is identified as a critical thermo-mechanical stress zone, where fluid-induced forces and thermally induced stresses jointly contribute to the initiation of mechanical damage in the heat exchanger tubes.

Furthermore, a significant increase in stress is observed at the tube bends, especially the inner tubes with higher bend angles. This phenomenon arises from the concentration of strain due to changes in flow direction, increased pressure gradients along the bend radius, and higher rates of temperature change in the inner tubes [15]. In other words, at bends, the combination of mechanical stress from flow redirection and thermal stress from temperature gradients leads to the formation of local critical points.

3.2. Thermal Analysis of the Feed-Gas Tube Bundle

As shown in Fig. 5. the thermal image clearly illustrates the performance of the first-stage feed-gas heat exchanger. The inlet air, at 141°C, enters the tube bundle header and, in the initial lines, experiences the steepest thermal gradient due to the significant temperature difference with the surrounding hot gases. The noticeable color change in the thermal contour from blue to green and yellow indicates a temperature rise of approximately 180°C in this region. As discussed in the thermal stress analysis, this section, due to the high rate of temperature change and substantial thermal difference, represents the most critical zone of the exchanger and requires careful design, material selection, and manufacturing methods to prevent thermal fatigue and mechanical damage. Along the flow path, heat transfer gradually stabilizes, and the air temperature increases uniformly, eventually reaching 422°C at the outlet header. This value is fully consistent with the design data and confirms the proper and efficient performance of the heat exchanger.

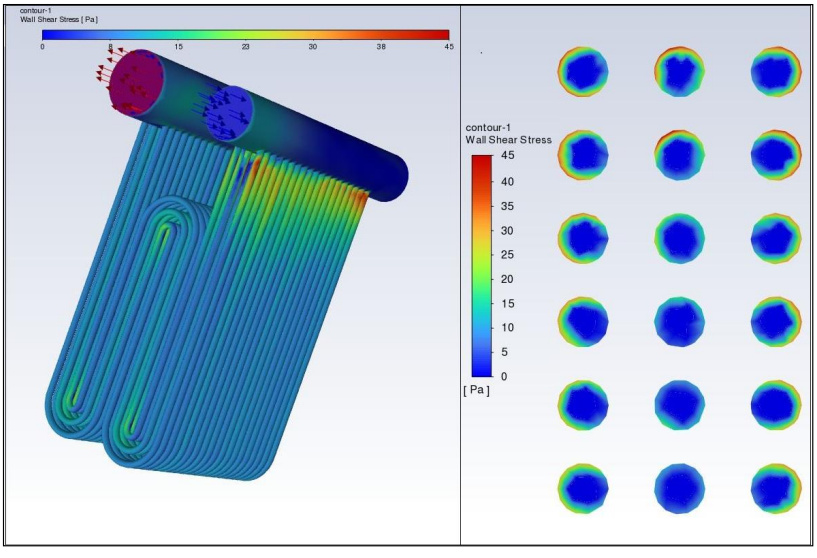

Fig. 3. Contours of Wall Shear Stress applied to the first-stage feed-gas tube bundle.

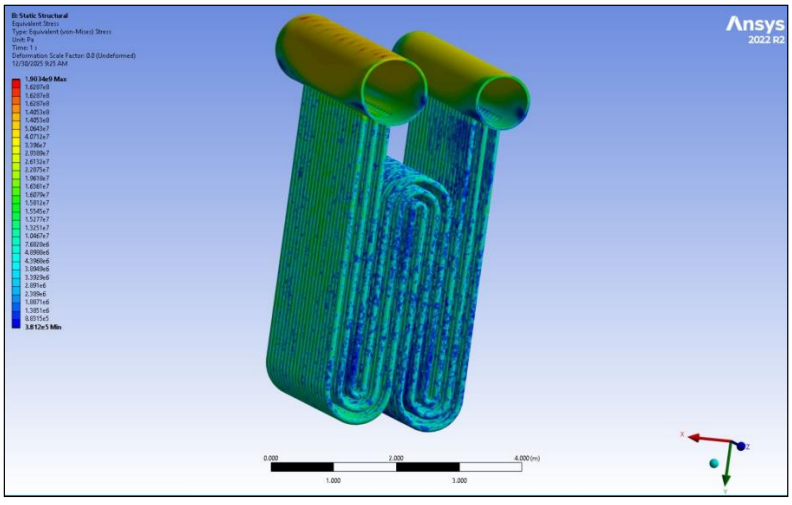

Fig. 4. Resulting structural von Mises stress distribution corresponding to the wall shear stress and thermal.

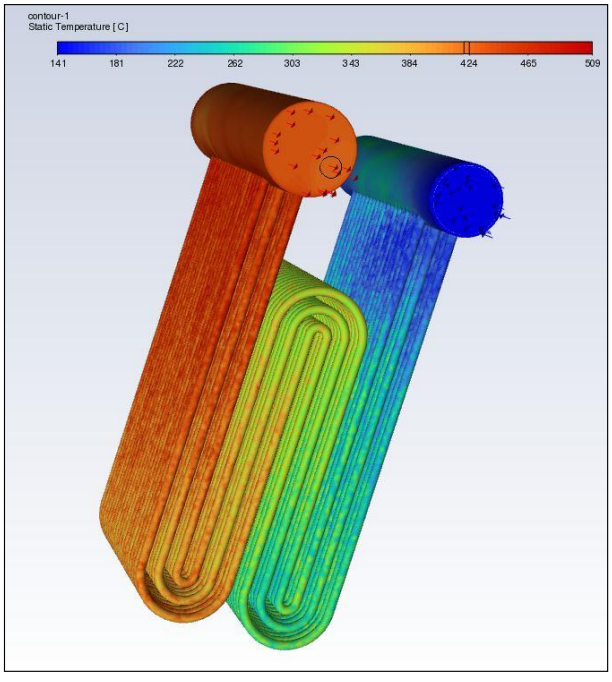

Fig. 5. Thermal analysis contours of the first-stage feed-gas tube bundle.

3.3. Velocity Vector Analysis

As shown in Fig. 6. the velocity vector analysis reveals that the velocity vectors are initially deflected toward the walls in the air inlet region connecting the header to the tube bundle, and the flow intensity increases in this zone. This velocity increase occurs precisely in the same critical region of the tube bundle previously identified as exhibiting the maximum shear stress, where the flow profile has not yet fully developed. This behavior results from the sudden reduction in flow cross-section from the header to the tubes, causing a local increase in velocity to satisfy mass conservation in compressible flow. Additionally, the pressure distribution and initial boundary-layer formation cause the flow profile to be non-uniform at the inlet; as the tube length increases and friction effects accumulate, the boundary layer develops, and the flow gradually reaches a uniform, fully developed profile [16].

3.4. Analysis of Total Deformation and Equivalent Elastic Strain

The superimposed results of the total deformation and equivalent elastic strain analyses indicate that the bend regions predominantly govern the mechanical response of the tube bundle. Both the maximum overall displacement and the highest concentration of elastic strain are observed at the inner radius of the tube bends. Elevated total deformation in these zones reflects restricted free thermal expansion and an asymmetric structural response caused by flow redirection and geometric constraints at the transition between straight and curved sections. Concurrently, the equivalent elastic strain contours confirm a localized amplification of elastic deformation, arising from the combined effect of thermal stresses, induced by steep temperature gradients between the tube interior and the surrounding hot gases, and mechanical stresses associated with pressure gradients and lateral fluid forces in the bends. The coincidence of peak strain with maximum deformation demonstrates that the bends act not only as regions of greater displacement but also as centers of strain-energy concentration, making them highly susceptible to thermo-mechanical fatigue initiation and cumulative damage. In contrast, the gradual reduction of both deformation and strain along the straight tube sections indicates a more uniform temperature field and a stabilized stress distribution. Accordingly, optimization of the bend

radius, improvement of temperature uniformity, and revision of support and expansion allowance conditions are identified as key measures to simultaneously reduce total deformation and elastic strain and enhance the service life of the tube bundle.

3.5. Field Inspection

To validate the simulation results, a sample of the first-stage feed-gas tube bundle was examined at the operational site. As shown in Fig. 8. field observations revealed that the damaged region corresponds exactly to the critical area identified in the simulation. This agreement indicates that the CFD model reliably predicted the zones with the highest thermal and shear stresses. The findings emphasize the importance of precise tube-geometry design and appropriate material selection to enhance the reliability, service life, and safety of heat exchangers in the direct-reduction ironmaking process.

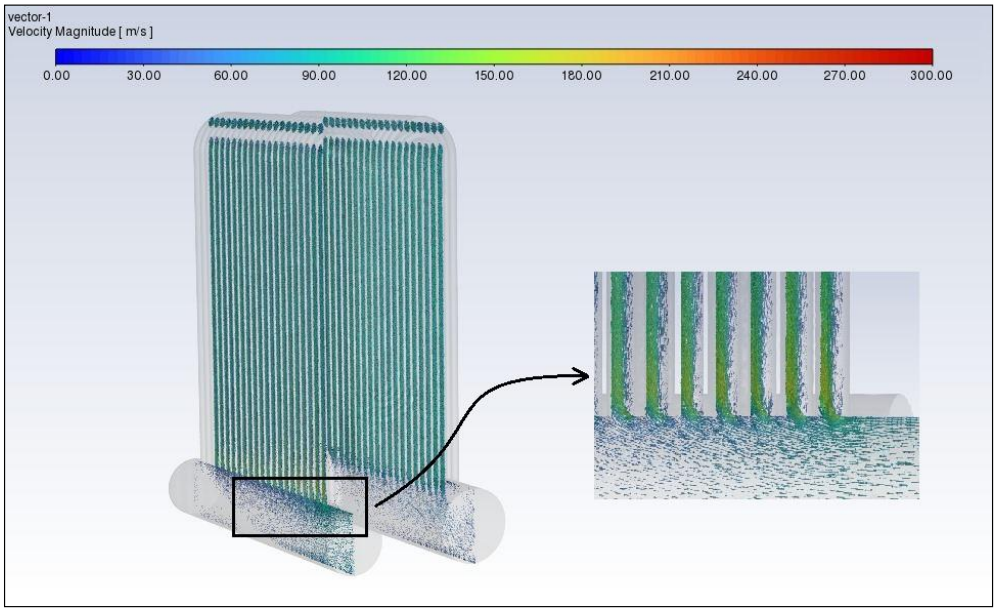

Fig. 6. Velocity vector analysis of the first-stage feed-gas tube bundle.

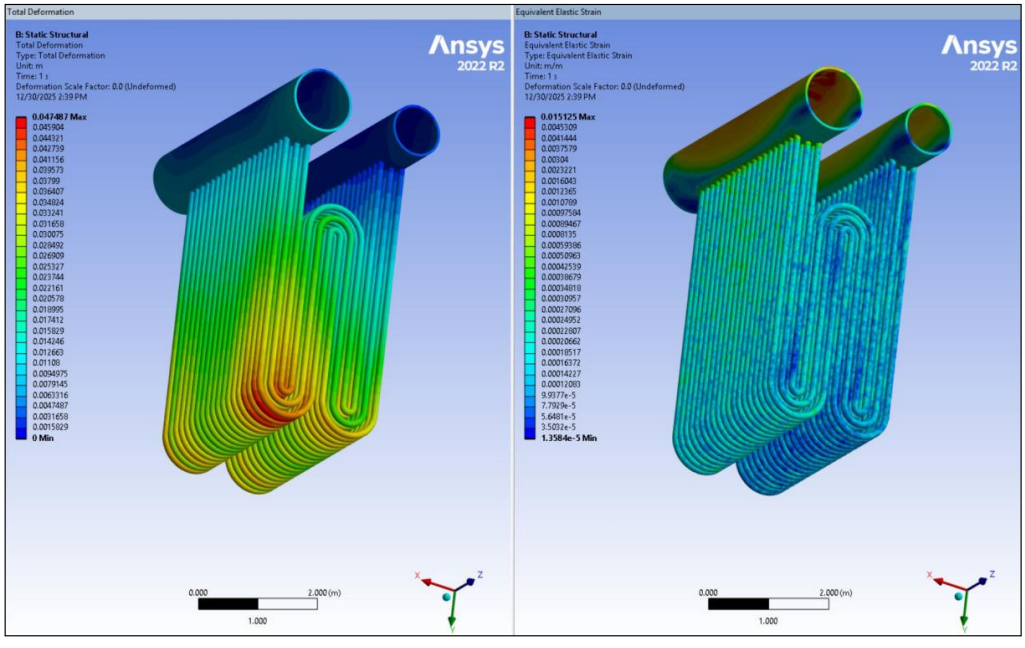

Fig. 7. Velocity vector analysis of the first-stage feed-gas tube bundle.

Fig. 8. Damaged sample of the first-stage feed-gas tube bundle.

4. Conclusions

The results of this study indicated that the first-stage feed-gas tube bundle in the Midrex process recuperator experiences the highest shear and thermal stresses in specific regions, particularly at the cold air inlet to the header and at the internal tube bends. Sudden geometric changes, significant temperature differences between the fluid inside the tubes and the heating gas, and local increases in flow velocity lead to stress concentration and the formation of critical zones. Numerical analysis using CFD, along with field inspection of damaged samples, confirmed the accurate identification of these regions and demonstrated full agreement with actual operational conditions. The findings highlighted the importance of precise geometric design, selection of creep- and oxidation-resistant materials, and optimization of operational parameters. Implementing corrective measures based on these results can enhance the tube bundle's service life, reduce operational downtime, and improve the recuperator's safety and efficiency in the direct reduction ironmaking process. In particular, the identified critical zones strongly suggest the need for optimized filleting (rounding) of the header-to-tube transition region to reduce local stress concentration, as well as the application of alloys with higher resistance to creep and thermal fatigue, especially for the first row of tubes exposed to the most severe thermo-mechanical loading.

References

[1] Bowen T.L, Guimond D.P, Muench R.K, Experimental investigation of gas turbine recuperator fouling, J Eng Gas Turbines Power. 1987; 109(3): 249-256.
[2] Mediokritskii E.L, Gaponov V.L, Loginov V.E, Study of heat transfer in recuperators by computer models, J Eng Phys Thermophys. 1997; 70: 119-124.
[3] Wojciech L, Daniel Z, Modification of a recuperator construction with CFD methods, Chem Process Eng. 2017; 38(4): 567-576.
[4] Gupta A, Roy S, Saha S, CFD analysis of a gas turbine recuperator with varying operating conditions, J Therm Sci Eng Appl. 2017; 9(2): 021009.
[5] Chun-Hsiang Y, Ming T, Chiun-Heng C, Chiun-Hsun C, Performance simulation and thermal stress analysis of ceramic recuperators formed by SiC and MAS, Numer Heat Transf A Appl. 2008; 7: 709-725.
[6] Yang L, Liu W, Zhang H, Wang Z, Experimental study on heat transfer characteristics of a ceramic recuperator for high-temperature applications, Energy Convers Manag. 2018; 171: 239-247.
[7] Krzysztof W, Simulation of deposit growth onto recuperator tubes in pit furnaces, Eng Trans. 2016; 64(4): 417-424.
[8] Marchionni M, Chai L, Bianchi G, Tassou S, Numerical modelling and transient analysis of a printed circuit heat exchanger used as recuperator for supercritical CO_2 heat to power conversion systems, Appl Therm Eng. 2019; 161: 114190.
[9] Patankar A, Deshpande A, Sapali S, Design and performance evaluation of a compact recuperator for a micro gas turbine, Energy Procedia. 2016; 90: 254-261.
[10] Kim J, Sibilli T, Ha M.Y, Kim K, Yoon S.Y, Compound porous media model for simulation of flat top U-tube compact heat exchanger, Int J Heat Mass Transf. 2019; 138: 1029-1041.
[11] Xie Y, Xu H, Zhang Y, Transient thermal modeling of a recuperator for waste heat recovery in steel production, Appl Therm Eng. 2018; 140: 475-484.
[12] Ghanbarpour M, Toghraie D, Optimization and simulation of a combined heat and power system with a recuperator for residential applications, Energy Rep. 2021; 7: 1895-1905.
[13] Hussain T, Rasul M, Khan M, Artificial neural network-based prediction of the performance of a gas turbine recuperator, Energy. 2020; 197: 117276.
[14] Emrehan G, Engin G, Alina A, A comprehensive numerical analysis on the thermo-hydraulic performance of U-bend tube with spherical dimple of shell-and-tube heat exchanger subjected to uniform/non-uniform magnetic fields, Int J Thermophys. 2024; 46.
[15] Krishna P, Alan I, Thermal stresses in U-bends, In: Mechanical Design of Heat Exchangers, 1984: 663-687.
[16] Minh Q, Benoit L, Mostafa S, Abdellah H, Jorge P, Features of transition to turbulence in sudden expansion pipe flows, Int J Heat Fluid Flow. 2019; 76: 187-196.